

Magnetic anisotropy of Fe/Pt (001) and Pt/Fe/Pt (001) using a first-principles approach

著者	Tsujikawa Masahito, Hosokawa Akihiko, Oda Tatsuki
journal or publication title	Physical Review B - Condensed Matter and Materials Physics
volume	77
number	5
page range	054413
year	2008-02-11
URL	http://hdl.handle.net/2297/11761

doi: 10.1103/PhysRevB.77.054413

Magnetic anisotropy of Fe/Pt(001) and Pt/Fe/Pt(001) using a first-principles approach

Masahito Tsujikawa, Akihiko Hosokawa, and Tatsuki Oda

Graduate School of Natural Science and Technology, Kanazawa University, Kanazawa 920-1192, Japan

(Received 23 August 2007; published 11 February 2008)

We investigated the magnetic anisotropy of an iron layer on a Pt(001) surface and some related systems by employing the local spin density approximation in a theoretical *ab initio* approach. We found that the surface system Pt/Fe/Pt(001) showed a perpendicular magnetic anisotropy and its anisotropy energy per iron atom amounted to a value which is 2 times larger than the value of bulk FePt. The surface relaxation much enhances the anisotropy energies, related to a large attractive force between the iron and platinum layers. A remarkable cap effect—that the covering platinum layer changes anisotropy energy—was also found to exist. We investigated the microscopic origin of the perpendicular anisotropy in relation to the local densities of states of the Fe atom. These quantities were discussed as a fingerprint of magnetic anisotropy in comparison with the results of the Fe chain at the step edge on a vicinal surface Pt(664). The atomic orbital magnetic moments were enhanced at the respective surface atoms.

DOI: [10.1103/PhysRevB.77.054413](https://doi.org/10.1103/PhysRevB.77.054413)

PACS number(s): 73.61.At, 75.70.-i, 75.30.Gw, 71.15.Rf

I. INTRODUCTION

Stable high-density magnetic recording media whose magnetic moment is perpendicular to surface or film plane have been required. Magnetic anisotropy is an important property for stability of the media. FePt and CoPt alloys are considered as good candidates of materials for developing a new medium in the next generation due to their large magnetic anisotropy energy (MAE).

Since the report of Gambardella *et al.*, in which they fabricated Co chains at step edges on Pt(997) surfaces using a self-assembly epitaxial technique and measured the magnetic properties,¹ the magnetism of the low-dimensional system with a supported material has been studied extensively.^{2,3} The system of Gambardella *et al.*, indeed, has been shown to have a perpendicular component for the magnetization easy axis. Realistic theoretical models for the step edge have been studied by several research groups, and they have obtained qualitative and semiquantitative agreement with the experimental results.^{4,5} Similar systems in which the Fe element is used instead of the Co element also have been studied experimentally^{3,6} and theoretically.^{7,8} In these studies, the perpendicular component for the magnetization easy axis has been also observed.

The easy axis of the above transition metal chain systems at the step edge on a Pt(997) surface specifies a direction which is perpendicular to the chain and canted by about 50° to the ascending step.^{1,9} This direction corresponds to one of the {001} directions in fcc Pt bulk or FePt regular alloy. Although in the previous works theoretical estimations of magnetic anisotropy explain the experimental results successfully, the origin in electronic structure for the magnetic anisotropy has not been discussed deeply.

In Fe-Pt and Co-Pt systems, it has been discussed that coordinated Pt atoms play important roles for their magnetic anisotropy. The hybridization with Fe (or Co) orbitals causes spin polarization on the Pt atom and, as a result, enhances the MAE due to a large spin-orbit coupling (SOC) in the Pt atom. The MAE is understood by two parts: a directional variation and an energy amplitude¹⁰—for example, MAE

$= E_0 + K_2 \sin^2(\Theta - \Theta_0)$. The control of parameters (K_2, Θ_0) would be desirable to one of the ends in the field of material magnetism. The results in experiments and theoretical approaches for decorations of magnetic materials to a surface imply an opportunity in which the system would be designed to have a controlled magnetic anisotropy.¹¹

We have found a strong perpendicular magnetic anisotropy (PMA) for a capped Fe overlayer on the Pt(001) surface, Pt/Fe/Pt(001). We will present results and discuss the magnetic anisotropy, compared with results of Fe overlayer on the Pt(111) surface.¹² This type of anisotropy enhancement has been pointed out in other systems—for example, Pd/Co/Pd(001).¹³ Recently, a similar system as Pt/Fe/Pt(001) has been fabricated and measured by x-ray magnetic circular dichroism, resulting in observations of hysteresis loops at a low temperature.¹⁴

We will also present results of the Fe chain at the step edge on a vicinal surface. The MAE of similar systems has been already studied in a systematic way and the perpendicular component has been found.^{7,8} Our results would be presented to see a relation with (001) surfaces on electronic structure and to confirm one that results from a pseudopotential electronic structure calculation and shows good agreement with those of the previous works which employed all-electron approaches.

II. MODELS AND METHOD

We considered surface systems of Fe/Pt(001) and Pt/Fe/Pt(001). The substrate has a (001) surface of fcc Pt bulk with four monolayers in our study. We assumed that the Fe atoms of overlayer sit on all the hollow sites of Pt(001) and the Pt capping layer also on the hollow sites of the Fe monolayer. The unit cell contains five (Fe, 4 Pt) and six (Fe, 5 Pt) atoms for Fe/Pt(001) and Pt/Fe/Pt(001) systems, respectively. In unrelaxed atomic structures, the nearest-neighbor distance in bulk FePt was used in our model for Fe-Pt distances, which is 5.11 a.u. compared with the distance to the Pt-Pt nearest neighbors (5.23 a.u.) in fcc Pt bulk

TABLE I. Layer distances (a.u.) and magnetic anisotropy energies (meV/Fe atom) in Fe/Pt(001) and Pt/Fe/Pt(001) for unrelaxed and relaxed cases, compared with the thin film Pt/Fe/Pt_{1 ML}(001) and the FePt bulk. The distances in parentheses specify the assumed data.

	Pt(c)-Fe	Fe-Pt(1)	Pt(1)-Pt(2)	$E[100]-E[001]$	$E[110]-E[001]$
Fe/Pt(001) (unrelaxed)		(3.52)	(3.70)	-0.030	-0.002
Fe/Pt(001) (relaxed)		3.20	3.84	0.19	0.13
Pt/Fe/Pt(001) (unrelaxed)	(3.52)	(3.52)	(3.70)	4.02	3.79
Pt/Fe/Pt(001) (relaxed)	3.28	3.47	3.85	5.20	5.13
Pt/Fe/Pt _{1 ML} (001) (unrelaxed)	(3.52)	(3.52)		8.29	8.43
Pt/Fe/Pt _{1 ML} (001) (relaxed)	3.21	3.21		7.51	7.70
FePt bulk				2.734, ^a 2.61 ^b	

^aReference 25.

^bReference 19.

($a=7.41$ a.u.). We made surface relaxations, assuming that the atomic positions of three Pt layers located at bottom of substrate were fixed. The capped system Pt/Fe/Pt(001) has a local structure similar to that of the bulk system FePt, implying that the magnetic anisotropy perpendicular to the surface has a same origin in both systems. A vacuum layer of about 14 a.u. thick was assumed.

We also considered a Fe chain at the step edge on Pt(664) surface, in which the x axis is taken along the chain parallel to $[1\bar{1}0]$ and the z axis along $[111]$. Our model calculated is similar to the previous works,^{7,8} but includes a larger number of atoms (Fe and 21 Pt atoms) in unit cell. All the atoms were fixed on the sites extracted from fcc Pt bulk.

The present work is based on a local spin density approximation¹⁵ in Kohn-Sham theory.¹⁶ We have employed a fully relativistic pseudopotential approach, which have been developed previously.¹⁷⁻¹⁹ The wave functions have the two-component spinor form²⁰ and are determined self-consistently with effects of SOC embedded in the pseudopotential,²¹ which is the main origin of magnetic anisotropy. Energy cutoffs of 30 and 300 Ry were taken for wave functions and densities, respectively.²² In surface relaxations we used the atomic forces deduced from the wave functions including SOC effects.

The MAE was estimated by the difference of total energies; the total energy $E[lmn]$ when the system is magnetized along the $[lmn]$ direction. In the present work we used a $24 \times 24 \times 1$ mesh in \mathbf{k} -point sampling for flat (001) surfaces and a $32 \times 6 \times 1$ mesh for the step edge system.²³ It is noted that the equilibrium distance between Fe and Pt layers is not sensitive to the magnetization direction. Therefore, in this work all MAEs were estimated with using a fixed atomic configuration for each system. In our scheme,^{19,20} the constraint for the magnetization direction is not completely imposed in every case. This shortcoming forced us to accept a small ambiguity of directional angle ($\sim 1^\circ$). The spin and orbital magnetizations on atoms were estimated in the sphere with the radius of 2.5 a.u. for both Fe and Pt atoms.¹⁹

For materials of the 3d transition metal series, structural properties could not remarkably depend on the SOC due to a smaller energy of the coupling, an order of 10 meV,²⁴ while the counterpart of the 5d transition metal series—for

example, in Pt—amounts to an order of 1 eV. Although this energy scale may influence bond lengths and lattice constants, the previous work did not indicate any remarkable effect of SOC on the lattice constant¹⁹ and the present work only showed a small effect on the layer distances (~ 0.01 a.u.).

The local density of states (LDOS) of Fe atoms, which will be used for analyzing the electronic anisotropy, essentially provides a dependence on the magnetization direction of the system. In this work, however, the LDOS was calculated from the z -polarized magnetization system to present an overall anisotropy around Fe atom.

III. RESULTS

A. Fe layer on the flat surface

The layer distances, both unrelaxed and relaxed ones, are tabulated in Table I. As a general property, the distance between Pt layers just below the Fe layer becomes larger than the bulk layer distance of Pt (amounting to +4%), while the Fe layer faced on vacuum is largely contracted to the substrate [amounting to -9% in Fe/Pt(001)]. In Pt/Fe/Pt(001) the surface layer is also contracted by 7%. These features of a surface contraction and an extension at the next distance between Pt layers are also observed in Fe layer on Pt(111).¹²

The MAEs are also tabulated in Table I. The capping system Pt/Fe/Pt(001) has much larger perpendicular MAEs, compared with the Fe/Pt(001) system. This indicates that the capping Pt plays an important role for a large MAE. The magnitudes of the large MAEs are larger than those of the bulk system and the Fe chain on Pt(111) in the previous work.¹² To confirm the role of the capping Pt layer, we also calculated the MAEs of a Fe monolayer sandwiched by Pt layers, Pt/Fe/Pt_{1 ML}(001), obtaining an increase of PMA. The unrelaxed Fe/Pt(001) surface has a weak in-plane anisotropy and the surface relaxation introduced a PMA. The surface relaxation also increased the PMA in Pt/Fe/Pt(001), while it decreased in the sandwiched system. The decrease of the latter may be related to an excess contraction of the surface Pt layers. The MAEs in Table I do not show any strong in-plane magnetic anisotropy.

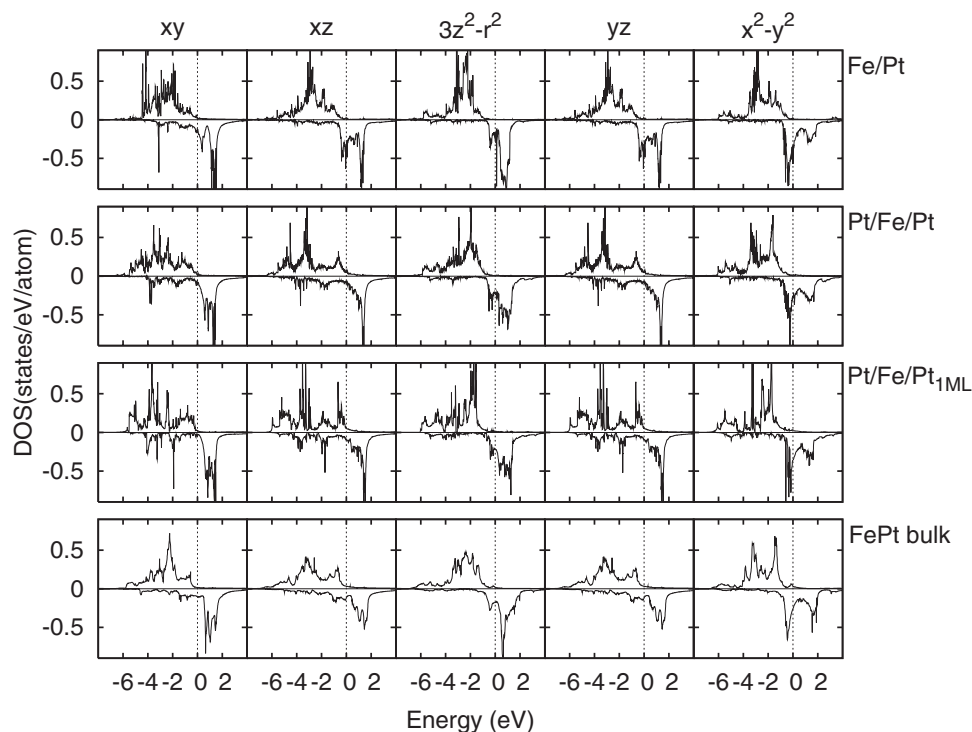


FIG. 1. The local density of states projected to the Fe components of d_{xy} , d_{xz} , $d_{3z^2-r^2}$, d_{yz} , and $d_{x^2-y^2}$ for the systems of Fe/Pt(001), Pt/Fe/Pt(001), Pt/Fe/Pt_{1ML}(001), and FePt bulk. At each panel, the majority and minority spin states are plotted up and down sides, respectively. The vertical dotted lines specify the Fermi level.

The LDOS provide information on properties of anisotropy in electronic structure. Figure 1 shows the LDOS which are projected to the Fe orbital local components of d_{xy} , d_{xz} , $d_{3z^2-r^2}$, d_{yz} , and $d_{x^2-y^2}$.¹² In Pt/Fe/Pt(001), effects of the capping Pt layer are remarkably observed around the Fermi level in the minority spin components of d_{xz} and d_{yz} , which are due to orbital hybridizations between the capping Pt and Fe atoms. These hybridizations lower the minority spin states of d_{xz} and d_{yz} of Fe/Pt(001) around the Fermi level, resulting in a low density of states at the Fermi level for d_{xz} and d_{yz} . Systems other than the Fe/Pt(001), which have the Fe layer sandwiched by Pt layers, show LDOS similar to each other in the respective d components. These LDOS are also similar to those of FePt bulk, as compared in Fig. 1. The above contrast between the systems with and without the capping Pt layer is related to the large difference in the property of MAEs (see Table I).

To consider this difference more from electronic structures, we present band dispersions of the Fe/Pt(001) and Pt/Fe/Pt(001) systems. The wave vectors were taken along connected lines, $\bar{\Gamma}-\bar{M}(\frac{\pi}{a}, \frac{\pi}{a})-\bar{X}(0, \frac{\pi}{a})-\bar{\Gamma}$ ($a=5.23$ a.u.). In Figs. 2(a) and 2(b), the magnetization dependence of the z and x axes is displayed, and in Figs. 2(c)–2(h) the character of local d components (d_{xy} , d_{xz} , $d_{3z^2-r^2}$, d_{yz} , and $d_{x^2-y^2}$) on Fe atom is assigned to band dispersions when the ratio of the component is larger than 10%. In the latter, the characters of the Fe orbitals, especially in Fe/Pt(001), are similar to the previous result of an isolated Fe layer.²⁴ It is found that the change by the existence of the capping Pt layer remarkably appears at the d_{xz} and d_{yz} components, as found in the LDOS.

The change of eigenvalues which is induced by a magnetization rotation contributes MAE. In Figs. 2(a) and 2(b), changes are observed along the lines presented. In Fig. 2(a) [Fe/Pt(001) system], the changes on the $\bar{X}-\bar{\Gamma}$ line seem to be relatively suppressed, while in Fig. 2(b) [Pt/Fe/Pt(001) system], the changes are remarkably observed below the Fermi level. As seen from Fig. 2, the portion where changes occur does not always have a character of Fe orbitals. This implies a considerable contribution from Pt atoms to MAE.

In Fig. 3, the characters of the capping Pt atom are presented on band dispersions as both majority and minority spin states for Pt/Fe/Pt(001) when the ratio of the component is larger than 5%. In Fig. 4, the same quantities of results are presented for Pt(1) as in Fig. 3. Both results of these figures are similar to each other. By comparing with Figs. 2(e)–2(h), for the characters of minority d_{xz} and d_{yz} spin states, clear hybridizations are observed between Fe and Pt. Comparing Figs. 3 and 4 with Fig. 2(b), the dispersion change by the magnetization rotation seems to originate from the Pt atoms which sandwich Fe layer rather than Fe atoms themselves. The result in Figs. 2–4 implies that a large amount of the MAE in Pt/Fe/Pt(001) comes from the Pt atoms. However, the perpendicularity of magnetic anisotropy in this system could not be determined by the Pt atoms themselves because the spin polarization on Pt is induced through the hybridization with Fe. Thus, it may be valid that the direction of the easy axis is mainly determined by the electronic structure of Fe atoms which is deformed by the surrounding Pt atoms, whereas the strength of magnetic anisotropy may be contributed from both Fe and Pt atoms.

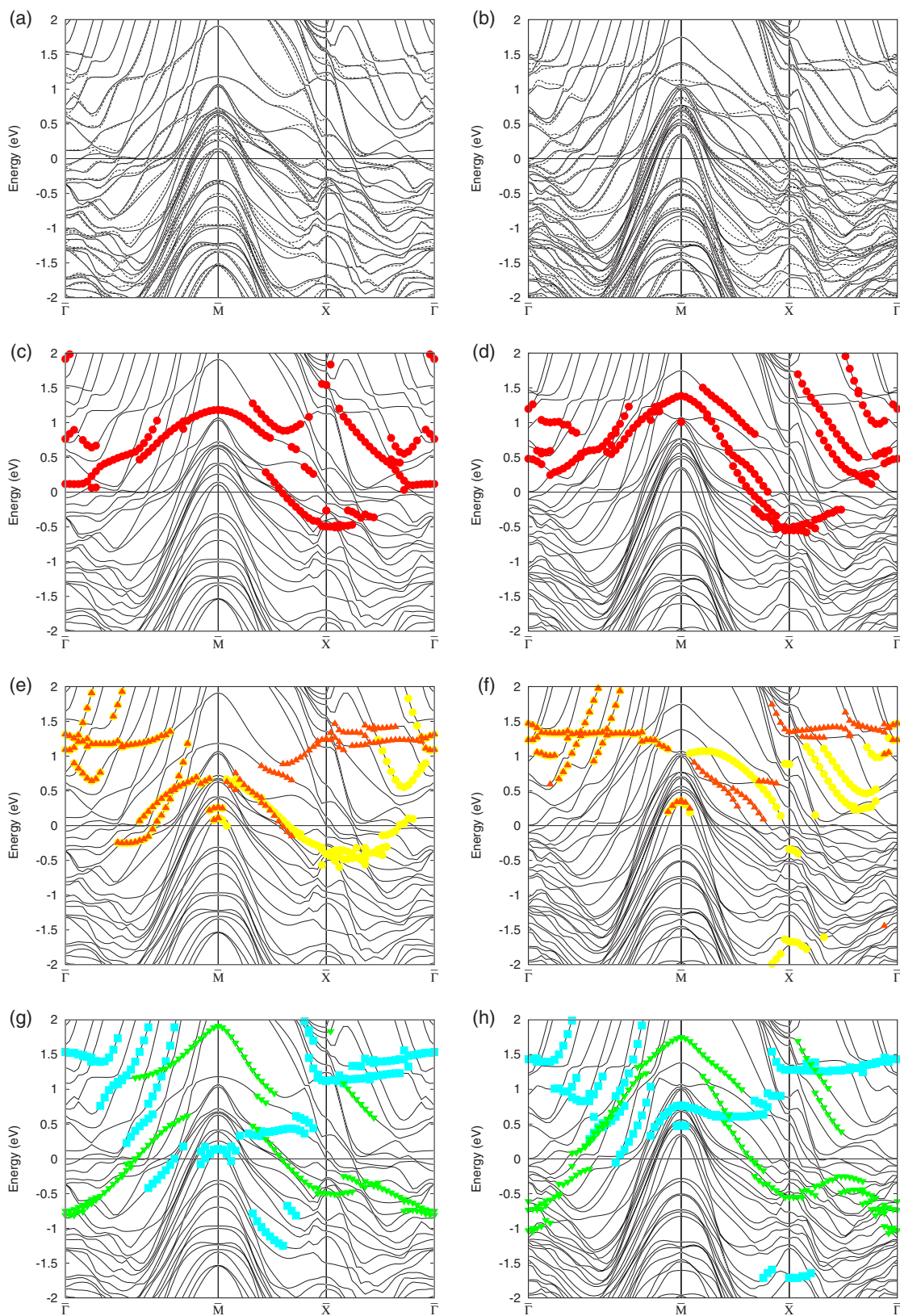


FIG. 2. (Color online) Band dispersions for the Fe/Pt(001) [(a), (c), (e), and (g)] and Pt/Fe/Pt(001) [(b), (d), (f), and (h)]. In the top panels, the magnetized direction dependence of the z axis (solid curves) and x axis (dashed curves) is shown. The Fe orbital local components of $d_{3z^2-r^2}$, d_{xz} , d_{yz} , d_{xy} , and $d_{x^2-y^2}$ for minority spin states are marked as red circles, orange triangles, yellow circles, blue squares, and green triangles, respectively. See text for other details.

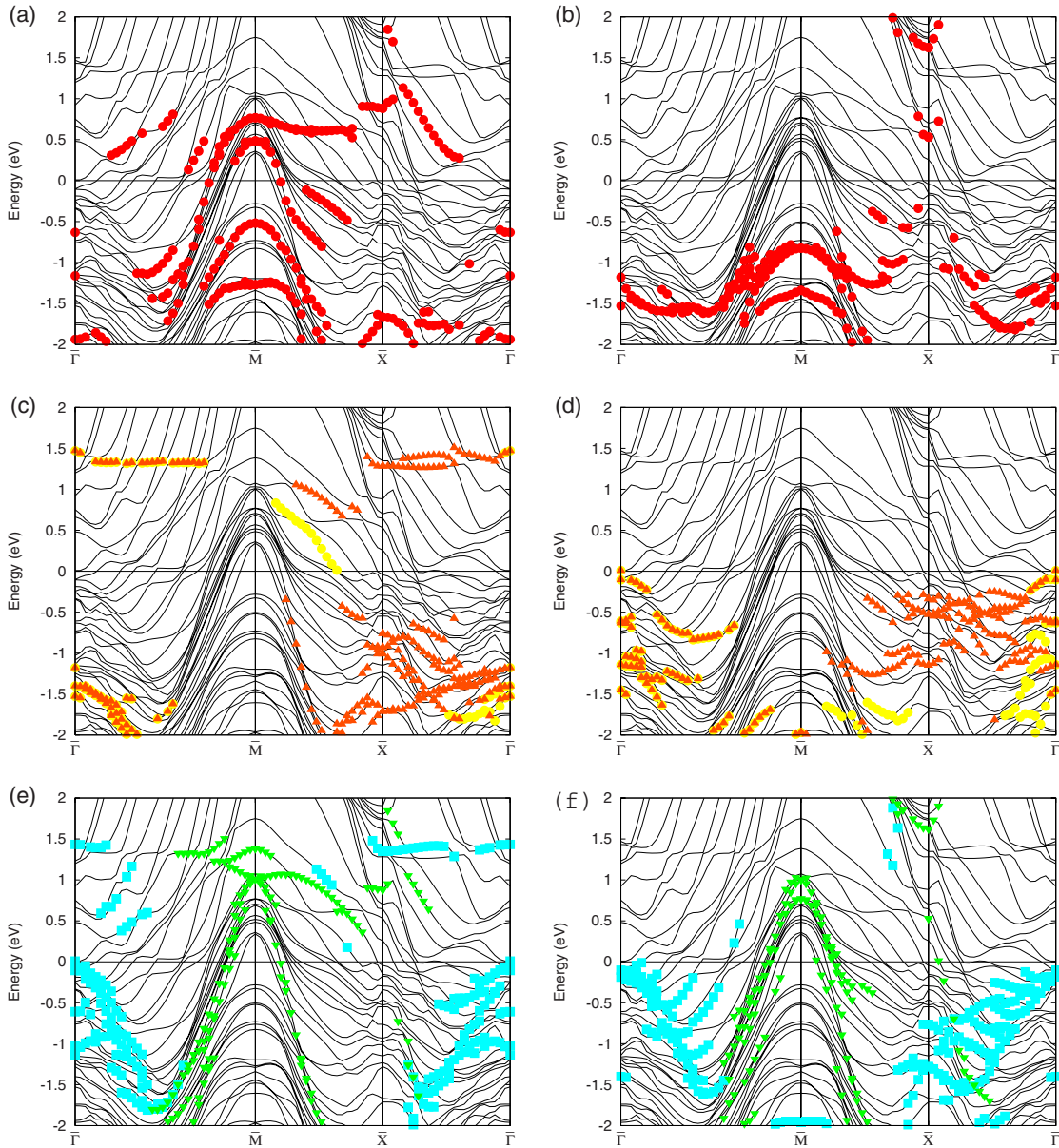


FIG. 3. (Color online) Band structure for the Pt/Fe/Pt(001) magnetized to the z axis. The minority (left) and majority (right) spin $d_{3z^2-r^2}$, d_{xz} , d_{yz} , d_{xy} , and $d_{x^2-y^2}$ states of the Pt(c) atom are marked as red circles, orange triangles, yellow circles, blue squares, and green triangles. See text for other details.

The origins of magnetic anisotropy have been discussed previously.²⁴ Daalderop *et al.*²⁶ summarized a couple of points: splittings by the SOC of partly occupied orbitally degenerate levels and second-perturbative contributions. Especially, the former contribution may be important at a high-symmetry point (or line) in \mathbf{k} space. It is rather difficult to estimate an individual contribution to MAE for candidates of symmetry points in Fig. 2(b). The latter is discussed below.

Though the SOC in Pt is larger, it may be valid to use a perturbative treatment of MAE. To discuss the essential magnetic features in Fe-Pt systems, we consider the minority spin state because the Fermi level sits in minority spin states for Fe local components. We consider a perturbative formula²⁴

$$E_x - E_z \sim \xi^2 \sum_{o,u} \frac{|\langle o | \ell_z | u \rangle|^2 - |\langle o | \ell_x | u \rangle|^2}{\epsilon_u - \epsilon_o}, \quad (1)$$

where o and u specify occupied and unoccupied minority spin states, respectively, and the ℓ_x and ℓ_z are angular momentum operators. The parameter of ξ is an average of SOC coefficients. The large ξ value for Pt is one of the reasons for large MAEs of CoPt and FePt alloys.^{25,27,28} The pair of occupied and unoccupied states around the Fermi level is important. In Fe-Pt systems, the Fermi level exists in minority spin states of Fe $3d$, which sensitively depends on the hybridizations among Fe $3d$ orbitals and with Pt $5d$ orbitals. These hybridizations largely affect the above matrix ele-

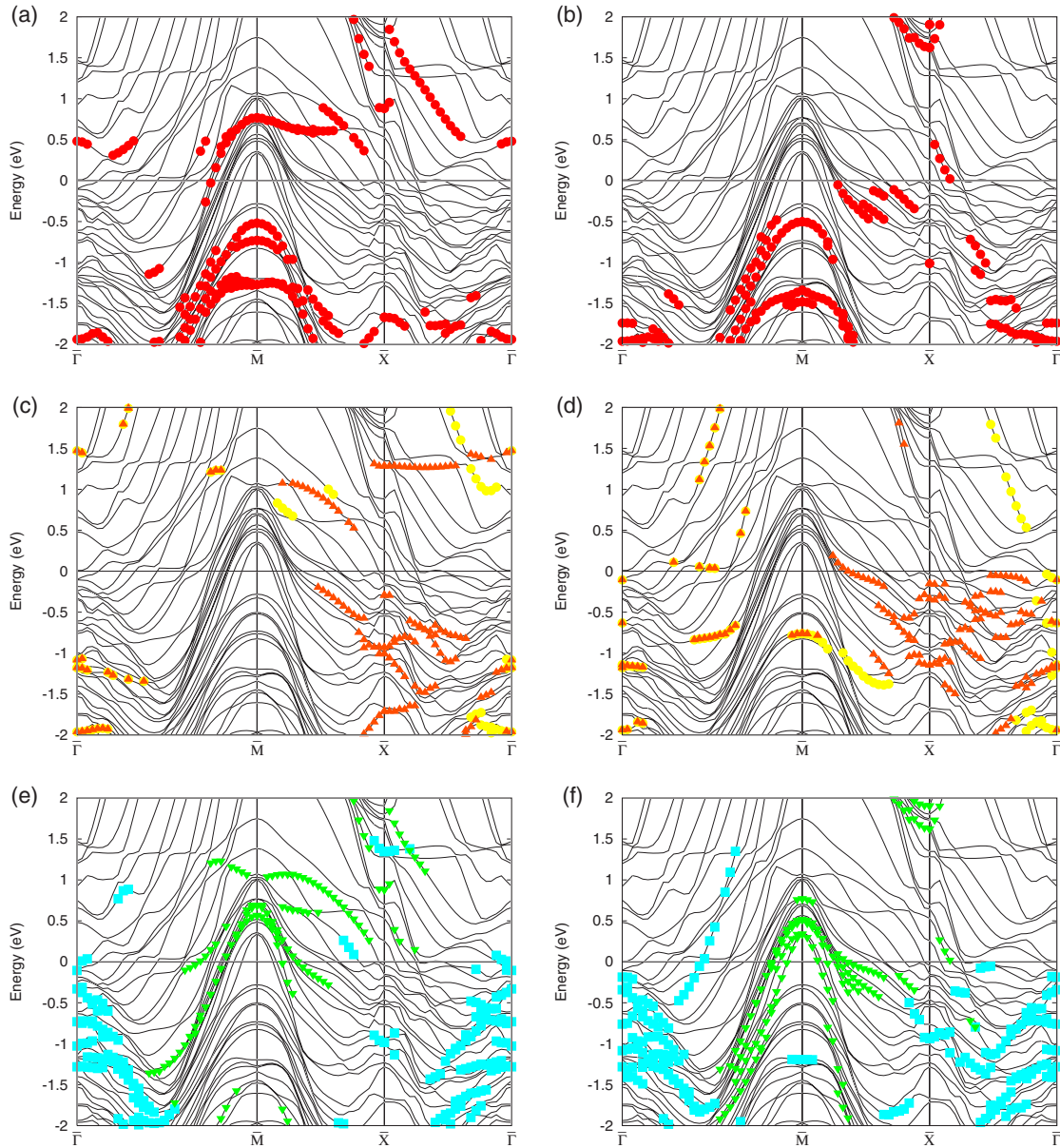


FIG. 4. (Color online) Band structure for the Pt/Fe/Pt(001) magnetized to the z axis. The minority (left) and majority (right) spin $d_{3z^2-r^2}$, d_{xz} , d_{yz} , d_{xy} , and $d_{x^2-y^2}$ states of the Pt(1) atom are marked as red circles, orange triangles, yellow circles, blue squares, and green triangles. See text for other details.

ments of ℓ_x and ℓ_z through changes of the orbitals on Fe atoms.

Taking into account the matrix elements of ℓ_x and ℓ_z , the change to the large perpendicular MAE in Pt/Fe/Pt(001) might be explained qualitatively by the remarkable reductions of d_{xz} and d_{yz} minority spin components at the Fermi level. Recently, it has been shown that the SOC coefficient at Pt atoms contributes a large contribution to the total MAE^{8,29} and a more strict analysis is required for clarifying the contribution of Pt atoms when one likes to estimate an atomic contribution by such a scheme as the present pseudopotential plane-wave method.

The atomic magnetic moments are presented in Table II, with the total spin magnetizations. The estimated values are almost consistent with the results of Fe-Pt systems which has

been studied theoretically in previous works on bulk and Fe/Pt(111) systems,^{19,25,28} while our results show a variation in atomic local structure. The total spin magnetization is increased in order of Fe/Pt(001), Pt/Fe/Pt(001), and Pt/Fe/Pt_{1 ML}(001). In contrast with this property, interestingly, the spin magnetic moments on Fe atom are not so changed against a variation of circumstance around the atom. The change of the total spin magnetization comes from the induced Pt spin moments which are generated by the 5d orbital hybridization with Fe 3d orbitals. The comparison of Pt layers in Pt/Fe/Pt(001) reveals that the capping-Pt spin moments are more induced than that of the Pt(1) layer. The spin moments on the Pt(2) layer are much smaller, compared with the Pt(1) layer.

TABLE II. Spin and orbital magnetic moments (μ_B) on the Fe and Pt atoms for the relaxed surfaces investigated. Pt(c), Pt(1), and Pt(2) represent the capping atom and the first and second nearest Pt atoms, respectively.

	Magnetization direction	Spin					Orbital			
		Total	Pt(c)	Fe	Pt(1)	Pt(2)	Pt(c)	Fe	Pt(1)	Pt(2)
Fe/Pt(001)	[100]	3.526		2.933	0.307	0.050		0.076	0.053	0.007
	[110]	3.525		2.933	0.307	0.049		0.076	0.053	0.007
	[001] easy axis	3.529		2.932	0.308	0.051		0.069	0.040	0.014
Pt/Fe/Pt(001)	[100]	3.641	0.349	2.962	0.256	0.009	0.100	0.028	0.040	0.010
	[110]	3.642	0.350	2.963	0.256	0.009	0.101	0.029	0.040	0.010
	[001] easy axis	3.632	0.342	2.957	0.252	0.006	0.058	0.036	0.032	0.005
Pt/Fe/Pt _{1 ML}	[100]	3.918	0.360	2.985	0.359		0.098	0.030	0.098	
	[110]	3.923	0.363	2.985	0.363		0.100	0.030	0.100	
	[001] easy axis	3.900	0.355	2.978	0.355		0.063	0.020	0.063	

The orbital magnetic moments on atoms have a variation depending on the location of atoms. The orbital moments on Fe are reduced from Fe/Pt(001) to Pt/Fe/Pt(001). The counterparts of Pt are much induced at the capping Pt site and reduced in the inner Pt one, similarly as mentioned above for the spin moments. In most cases, interestingly, the orbital moments of Pt atoms are reduced for the magnetization easy axis (or enhanced for the hard axes).

Orbital magnetic moments of surface atoms in Pt/Fe/Pt(001) and Fe/Pt(001) are interestingly compared with those in the Fe/Pt(111) and Fe-chain/Pt(111) for which the in-plane magnetic anisotropies were obtained previously. Figure 5 presents the orbital magnetic moments in systems of various anisotropies which are from a strong PMA to a strong in-plane one. The Pt/Fe/Pt(001) of strong PMA have smaller values on the Fe atom and larger ones for the surface Pt atom. Even in the other systems, the orbital moments of surface atom are larger than that of inner layers. The moment on Fe of Fe-chain/Pt(111) for the system spin polarized along the chain is largest in Fig. 5.

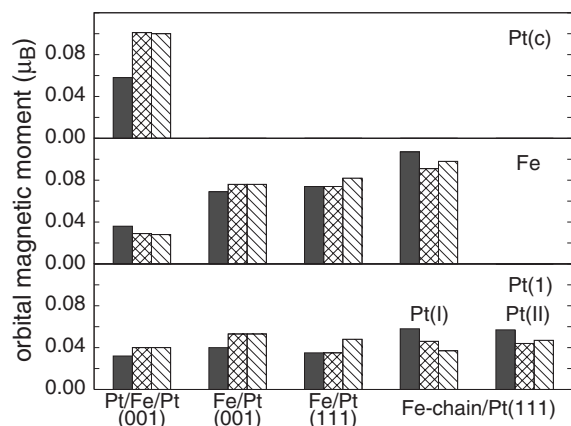


FIG. 5. Orbital magnetic moments of Fe and Pt atoms, as a variation of magnetic anisotropy; strong perpendicular anisotropy on the left-hand side of figure. The data at Pt(111) surfaces are cited from Ref. 12. The dark-hatched bars are of the easy axis, and the cross-hatched and line-hatched bars are of the hard axes.

B. Fe chain at the step edge

The isolated Fe chain which has the atomic distance when deposited on a Pt(111) surface has been shown to have a magnetization easy axis along the chain.^{30,31} At the step edge that is constituted by a couple of neighboring (111)-surface terraces, the Fe chain has an out-of-plane component for the magnetization easy axis in the theoretical approaches.^{7,8} The magnetization direction dependence of the total energy for Fe-chain/Pt(664) is presented in Fig. 6, compared with results of the previous theoretical all-electron approaches. The direction along the Fe chain is one of the magnetization hard axes, which has been pointed out in previous works.³² This result makes a remarkable contrast with the easy axis along the chain in our previous result about Fe-chain/Pt(111).¹² The difference is attributed to the existence of the Pt atoms located beside the Fe chain in the Fe-chain/Pt(664) system. The easy axis is canted by 50° from the z axis in the yz plane, and the anisotropy constant was estimated to be 1.19 meV per iron atom, resulting in $E(\phi) - E(0) = 0.51 - 1.19 \cos^2(\phi + 50)$ meV per iron atom where ϕ is defined as

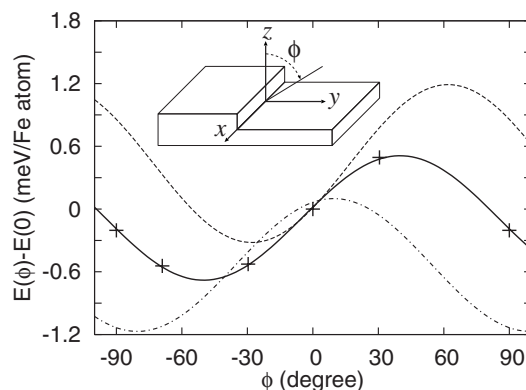


FIG. 6. Magnetization direction dependence of total energy $E(\phi) - E(0)$, where ϕ measures the angle from the z axis to the y axis in the yz plane. The present work is specified by the crosses (calculated data) and the solid curve [fitted to $E(\phi) - E(0) = 0.51 - 1.19 \cos^2(\phi + 50)$], the results of all-electron approaches by the dashed (Ref. 7) and dot-dashed (Ref. 8) curves.

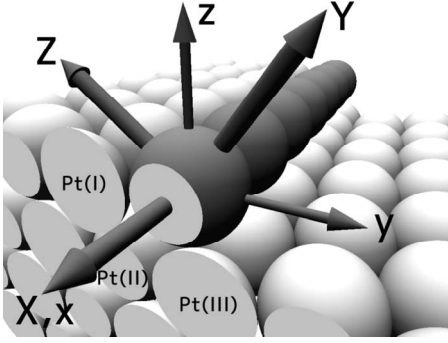


FIG. 7. The local coordinate system that the X axis is along the chain ($[1\bar{1}0]$) and Z axis is parallel to the $[001]$ direction.

the azimuth angle. The anisotropy constant agrees with the values of all-electron approaches, 1.51 and 1.27 meV per iron atom.^{7,8} The direction of the easy axis ($\phi=-50^\circ$) is in between the previous values, $\phi=-28^\circ$ and -80° .^{7,8}

The system of Fe-chain/Pt(664) has three types of Pt atoms nearest to the Fe atom; at the upper terrace, in the substrate bulk, and at the lower terrace, labeled by Pt(I), Pt(II), and Pt(III), respectively (see Fig. 7). The spin magnetic moment on the Fe atom is $3.12\mu_B$ and those on Pt(I), Pt(II), and Pt(III) are $0.15\mu_B$, $0.11\mu_B$, and $0.14\mu_B$. These values are almost the same as the previous linear muffin-tin orbital (LMTO) result³³ while they are smaller by about half than those of Pt atoms near the Fe atoms presented in Table II. This is because the present system with the step edge is unrelaxed and the increase of hybridizations between Fe and Pt orbitals may enhance the spin moments on Pt atoms in a relaxed system which results in shorten atomic distances between Fe and Pt atoms.

We also estimated orbital moments on Fe atom for the Fe chain system, as shown in Table III. When the total spin magnetization was fixed to perpendicular direction ($\theta=90^\circ$, $\phi=0^\circ$), the orbital moment on Fe atom ($0.124\mu_B$) has an almost same value as estimated by Shick *et al.* ($0.12\mu_B$).⁷ In the system of Fe-chain/Pt(664), the orbital moment on Fe atom for the total spin magnetization fixed to the x axis ($\theta=0^\circ$) was smaller than those fixed to the y or z axis. When the total spin magnetization was rotated to the y or z axis, the orbital moment on Fe atom, as well as the case of Co chain,⁷ has been found to have a component perpendicular to the spin magnetization.^{4,34} In our calculation this canting of the

orbital moment was also observed in both Fe-chain/Pt(664) and Fe-chain/Pt(111). Our angles of $\phi=104^\circ$ (second row in Table III) and $\phi=-2^\circ$ (third row in Table III) are similar to 97° and -1° in the previous study.⁷

IV. DISCUSSIONS

For the Co chain at the step edge, the direction of easy axis was found to take values of -51° and $\phi=-42^\circ$.^{5,9} A similar situation was also obtained for the Fe chain. In the present work the easy axis was found at $\phi=-50^\circ$. It would be interesting to compare it with the (001) surface on a magnetic property, because the easy axis is almost along to a $[001]$ direction ($\phi=-55^\circ$). This direction is presented by the Z axis of the local coordinate in Fig. 7, showing the X and Y axes ($[1\bar{1}0]$ and $[110]$). In Fig. 8, we display the LDOS of the Fe atom for the systems of Fe-chain/Pt(111) and Fe-chain/Pt(664) by using the local coordinate XYZ system. In Fe-chain/Pt(664) the d_{xz} component for the minority spin state around the Fermi level is decreased from the counterpart for Fe-chain/Pt(111). This is due to existence of the Pt atoms at the upper terrace near the Fe atom. As mentioned previously a similar decrease observed for the d_{xz} component around the Fermi level when the Fe/Pt(001) surface was capped with Pt atoms (see Fig. 1). For the systems of Fe-chain/Pt(111) and Fe-chain/Pt(664), the minority spin state for d_{yz} component at the vicinity of the Fermi level is pushed up to above the Fermi level. Additionally, the minority spin components of d_{xy} and $d_{x^2-y^2}$ seem to correspond to those of $d_{x^2-y^2}$ and d_{xy} in Pt/Fe/Pt(001). As a result, the minority spin states around Fermi level in Fe-chain/Pt(664) effectively give rise to a magnetic anisotropy along the Z axis.

Repetto *et al.* investigated the magnetic anisotropy of Fe thin films on Pt(111) and Pt(997) surfaces.⁶ Through their experiment, it was concluded that the magnetization easy axis of the Fe monoatomic chain on the Pt(997) step edge was perpendicular to the chain and the angle ϕ was about -80° . As concluded in the system of Co chain on the Pt(664) step edge, the easy axis might be expected to be canted to the film plane by the surface relaxation.^{5,35}

Recently, Imada *et al.* fabricated the thinnest limit of $L1_0$ -ordered FePt film which consists of Fe monolayer sandwiched by Pt(001) layers and observed that the film has a PMA.¹⁴ This system corresponds well to our system studied except for the numbers of the substrate and capping layers.

TABLE III. Atomic spin and orbital magnetic moments (μ_B) on Fe atom for Fe-chain/Pt(664), compared with Fe-chain/Pt(111). The respective moments for the systems spin-polarized parallel to the chain ($\theta=0^\circ$), perpendicular to the chain within the surface ($\theta=90^\circ$, $\phi=90^\circ$), and perpendicular to the (111) terrace ($\theta=90^\circ$, $\phi=0^\circ$) are given.

Spin magnetization direction	Fe-chain/Pt(111)									Fe-chain/Pt(664)					
	θ ϕ		Spin			Orbital			Spin			Orbital			
			m_s	θ	ϕ	m_o	θ	ϕ	m_s	θ	ϕ	m_o	θ	ϕ	
x	0	—	3.043	0		0.107	0		3.120	0		0.092	0		
y	90	90	3.045	90	90	0.091	90	70	3.120	90	91	0.113	90	104	
z	90	0	3.045	90	0	0.098	90	18	3.120	90	-1	0.124	90	-2	

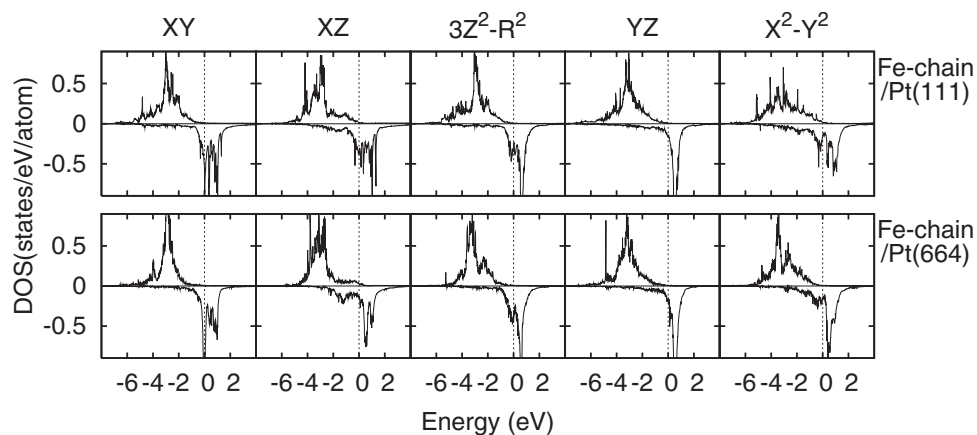


FIG. 8. The local density of states projected onto the Fe components of d_{XY} , d_{XZ} , $d_{3Z^2-R^2}$, d_{YZ} , and $d_{X^2-Y^2}$ for the systems of Fe-chain/Pt(111) and Fe-chain/Pt(664).

The experimental evidence of PMA might be confirmed by our theoretical calculations. The latter notes that the sandwiched local structure is important for the PMA. While the effects of the substrate may be almost included by judging from a convergence test of MAEs with respect to the number of layers in the substrate,³⁶ the number of capping layers also influences the MAE. The comparison between the results of Pt/Fe/Pt(001) and Pt/Fe/Pt_{1 ML}(001) calls a decrease of MAE with respect to the number of capping layers, as was found in the system Cu/Co/Cu(001).^{37,38} Indeed, an additional capping layer reduced the MAE of $E[100]-E[001]$ to 1.2 meV per iron atom, but the PMA has been kept in the system. The experimental Fe magnetic moment in the thin films seems to be slightly reduced from the bulk value.¹⁴ Correspondingly, both the spin and orbital magnetic moments estimated in our system Pt/Fe/Pt(001) ($2.96\mu_B$ and $0.036\mu_B$) were decreased, compared with the respective bulk values ($3.02\mu_B$ and $0.067\mu_B$).¹⁹

The theoretical approach which uses a local density approximation¹⁵ (LDA) usually underestimates orbital magnetic moments and MAEs. This is due to missing an explicit orbital splitting in the theory. This effect should be contained in electron correlations, and several approaches have been performed to improve such a drawback in a usual LDA. The explicit artificial introduction of an orbital polarization³⁹ was discussed for a FePt bulk system and the LDA+U approach was also performed to improve the absolute values of orbital magnetic moments and MAEs.^{25,40}

V. CONCLUSION

In summary, we have estimated the MAE for the Fe/Pt(001) and Pt/Fe/Pt(001) surfaces. The latter showed a large perpendicular MAE. It was found that the capping Pt layer much enhanced a perpendicular component of magnetic anisotropy and the atomic relaxation also enhanced it with strong promotions of hybridization between the Fe $3d$ and Pt $5d$ orbitals. The analysis of LDOS and band dispersion revealed that the PMA was induced with accompanying

a remarkable reduction of the d_{xz} and d_{yz} components at the Fermi level. We presented the magnetic anisotropy of Fe chain at the Pt(664) step edge. Our result by employing pseudopotentials showed good agreement with the results of all-electron approaches. The magnetic properties of the vicinal surface were compared with those of the flat Pt(111) surface. The observation in the LDOS, that the d_{XZ} component at the Fermi level was reduced, indicated that the Pt(I) atom beside the Fe chain played a role of enhancement for the magnetic anisotropy parallel to the $[001]$ in the local coordinate. The present work implies that the capping Pt atoms possibly increase a magnetic anisotropy to a local $[001]$ direction.

We also estimated the spin and orbital magnetic moments. For the system of Fe-chain/Pt(664), the spin and orbital magnetic moments well agree with the results of previous works. It was found that the orbital moment which faces to the vacuum seemed to be enhanced. In the Fe overlayer capped by Pt layer [Pt/Fe/Pt(001)] the orbital moments on Fe were remarkably reduced. The orbital moments were discussed in a variation of the magnetic anisotropies observed for some local atomic structures.

Experiences encountered in the present work contain relationships between magnetic anisotropies and local structures of the Fe-Pt system. This information is useful for understanding the decorated magnetic surface system in experiments and could be building blocks for a material design.

ACKNOWLEDGMENTS

The computation in this work was carried out using the facilities of the Supercomputer Center, Institute for Solid State Physics, University of Tokyo. This work has been partially supported by the Japan Society for the Promotion of Science (JSPS) under Project No. 16310081. One of the authors (T.O.) would like to thank the JSPS for financial support (Grants No. 17510097, No. 17540292, and No. 19048002).

- ¹P. Gambardella, A. Dallmeyer, K. Maiti, M. C. Malagoli, W. Eberhardt, K. Kern, and C. Carbone, *Nature (London)* **416**, 301 (2002).
- ²P. Gambardella, S. Rusponi, M. Veronese, S. S. Dhési, C. Grazioli, A. Dallmeyer, I. Cabria, R. Zeller, P. H. Dederichs, K. Kern, C. Carbone, and H. Brune, *Science* **300**, 1130 (2003).
- ³R. Cheng, K. Y. Guslienko, F. Y. Fradin, J. E. Pearson, H. F. Ding, D. Li, and S. D. Bader, *Phys. Rev. B* **72**, 014409 (2005).
- ⁴A. B. Shick, F. Maca, and P. M. Oppeneer, *Phys. Rev. B* **69**, 212410 (2004).
- ⁵S. Baud, Ch. Ramseyer, G. Bihlmayer, and S. Blugel, *Phys. Rev. B* **73**, 104427 (2006).
- ⁶D. Repetto, T. Y. Lee, S. Rusponi, J. Honolka, K. Kuhnke, V. Sessi, U. Starke, H. Brune, P. Gambardella, C. Carbone, A. Enders, and K. Kern, *Phys. Rev. B* **74**, 054408 (2006).
- ⁷A. B. Shick, F. Maca, and P. M. Oppeneer, *J. Magn. Magn. Mater.* **290-291**, 257 (2005).
- ⁸M. Komelj, D. Steiauf, and M. Fahnle, *Phys. Rev. B* **73**, 134428 (2006).
- ⁹B. Ujfalussy, B. Lazarovits, L. Szunyogh, G. M. Stocks, and P. Weinberger, *Phys. Rev. B* **70**, 100404(R) (2004).
- ¹⁰P. Bruno, *Phys. Rev. B* **39**, 865 (1989).
- ¹¹S. Rusponi, T. Cren, N. Weiss, M. Epple, P. Bulushek, L. Claude, and H. Brune, *Nat. Mater.* **27**, 546 (2003).
- ¹²M. Tsujikawa, A. Hosokawa, and T. Oda, *J. Phys.: Condens. Matter* **19**, 365208 (2007); **19**, 479002 (2007).
- ¹³D. S. Wang, R. Wu, and A. J. Freeman, *Phys. Rev. B* **48**, 15886 (1993).
- ¹⁴S. Imada, A. Yamasaki, S. Suga, T. Shima, and K. Takanashi, *Appl. Phys. Lett.* **90**, 132507 (2007).
- ¹⁵J. P. Perdew and A. Zunger, *Phys. Rev. B* **23**, 5048 (1981).
- ¹⁶P. Hohenberg and W. Kohn, *Phys. Rev.* **136**, B864 (1964); W. Kohn and L. J. Sham, *Phys. Rev.* **140**, A1133 (1965).
- ¹⁷G. Theurich and N. A. Hill, *Phys. Rev. B* **64**, 073106 (2001).
- ¹⁸A. Dal Corso and A. M. Conte, *Phys. Rev. B* **71**, 115106 (2005).
- ¹⁹T. Oda and A. Hosokawa, *Phys. Rev. B* **72**, 224428 (2005).
- ²⁰T. Oda, A. Pasquarello, and R. Car, *Phys. Rev. Lett.* **80**, 3622 (1998).
- ²¹D. Vanderbilt, *Phys. Rev. B* **41**, 7892 (1990).
- ²²K. Laasonen, A. Pasquarello, R. Car, C. Lee, and D. Vanderbilt, *Phys. Rev. B* **47**, 10142 (1993).
- ²³H. J. Monkhost and J. D. Pack, *Phys. Rev. B* **13**, 5188 (1976).
- ²⁴D. S. Wang, R. Wu, and A. J. Freeman, *Phys. Rev. B* **47**, 14932 (1993).
- ²⁵P. Ravindran, A. Kjekshus, H. Fjellvag, P. James, L. Nordstrom, B. Johansson, and O. Eriksson, *Phys. Rev. B* **63**, 144409 (2001).
- ²⁶G. H. O. Daalderop, P. J. Kelly, and M. F. H. Schuurmans, *Phys. Rev. B* **50**, 9989 (1994).
- ²⁷G. H. O. Daalderop, P. J. Kelly, and M. F. H. Schuurmans, *Phys. Rev. B* **44**, R12054 (1991).
- ²⁸A. Sakuma, *J. Phys. Soc. Jpn.* **63**, 3053 (1994).
- ²⁹S. Baud, Ch. Ramseyer, G. Bihlmayer, S. Blugel, C. Barreateau, M. C. Desjonqueres, D. Spanjaard, and N. Bernstein, *Phys. Rev. B* **70**, 235423 (2004).
- ³⁰Y. Mokrousov, G. Bihlmayer, and S. Blugel, *Phys. Rev. B* **72**, 045402 (2005).
- ³¹Isolated Fe chains show a change in their easy axis at a shorter atomic distance, which was discussed in the following reference: G. Autes, C. Barreateau, D. Spanjaard, and M.-C. Desjonqueres, *J. Phys.: Condens. Matter* **18**, 6785 (2006).
- ³²The energy difference of $E_x - E_z$ was estimated to be 1.21 meV per iron atom, compared with 2.3 and 2.8 meV in Refs. 7 and 8, respectively.
- ³³C. Ederer, M. Komelj, and M. Fahnle, *Phys. Rev. B* **68**, 052402 (2003).
- ³⁴L. M. Sandratskii, *Adv. Phys.* **47**, 91 (1998).
- ³⁵F. Maca, A. B. Shick, J. Redinger, and P. M. Oppeneer, *Czech. J. Phys.* **56**, 51 (2006).
- ³⁶In our convergence test with respect to the number of substrates, four Pt monolayers reproduce the MAEs of eight Pt monolayers in both Fe/Pt(111) and Pt/Fe/Pt(001) systems with an accuracy within 15%. The following reference for Fe/W(110) is also interesting: T. Andersen and W. Hubner, *Phys. Rev. B* **74**, 184415 (2006).
- ³⁷P. Krams, F. Lauks, R. L. Stamps, B. Hillebrands, and G. Guntherodt, *Phys. Rev. Lett.* **69**, 3674 (1992).
- ³⁸R. Wu and A. J. Freeman, *J. Magn. Magn. Mater.* **200**, 498 (1999).
- ³⁹O. Eriksson, M. S. S. Brooks, and B. Johansson, *Phys. Rev. B* **41**, 9087 (1990).
- ⁴⁰A. B. Shick and O. N. Mryasov, *Phys. Rev. B* **67**, 172407 (2003).